Mobilities of Labeled and Unlabeled Single-Stranded DNA in Free Solution Electrophoresis

A. R. Völkel

Department of Physics, University of Toronto, Toronto, Ontario, Canada M5S 1A7

J. Noolandi*

Xerox Research Centre of Canada, 2660 Speakman Drive, Mississauga, Ontario, Canada L5K 2L1

Received May 5, 1995; Revised Manuscript Received July 21, 1995[⊗]

ABSTRACT: Flexible polyelectrolytes of different sizes cannot be separated by free solution electrophoresis beyond a certain length exceeding a few monomers. The reason for this size-independent mobility is the equal scaling of the drag and driving forces with the molecular size. By selectively modifying the polyelectrolytes, this scaling symmetry can be broken and a size-dependent mobility can be achieved. We investigate the mobility of short flexible polyelectrolytes, such as single-stranded DNA, with and without a neutral label the size of a single nucleic acid. Numerical simulations allow us a systematic study of the microscopic dynamics of these systems and the impact of the neutral label, which is used to break the initial scaling symmetry, on the mobility. We find a free rotation of all the polyelectrolytes under investigation due to thermal fluctuations (this is in contrast to double-stranded DNA, where the fluctuations are less important due to its larger mass and charge per persistence length and where alignment with the external field has been observed). The impact of the neutral label can be observed as a systematic decrease of the mobility which becomes less pronounced for increasing total molecular size. This suggests that attaching a short neutral label will not allow for single base resolution of single-stranded DNA in free solution. On the other hand, the shift of the mobility due to the neutral label can be significant enough to utilize this method as diagnostic tool by specifically labeling only single-stranded DNA fragments with desired properties. Free solution electrophoresis experiments using single-stranded DNA fragments and biotin and trimethoxytrityl modifications as neutral labels confirm the numerical results.

I. Introduction

Electrophoresis has proven to be a useful method in chemistry and biology to separate polymers of different lengths. At present, it is a very important tool in separating nucleic acids from very short sizes up to a few megabases. Nucleic acids are flexible polyelectrolytes (for molecular sizes larger than their persistence length) and behave like free draining coils in free solution; i.e., their migration speed in this case is independent of their size.[1] Separation is achieved by performing electrophoresis in restricted media such as gels or polymer solutions.[2,3] While this is quite an efficient method (e.g., in polyacrylamide gels, single-stranded DNA can be separated up to a few hundred; with the use of pulsed fields up to one thousand, bases with a resolution of one base), the time necessary to perform a single run is quite long. In special cases, e.g., if one wants to detect nucleic acid fragments with a well-defined characteristic rather than separating by size, faster separation techniques based on free solution electrophoresis are desirable.

In this paper, we investigate electrophoresis of short, single-stranded nucleic acids or nucleic acid−protein complexes in free solution. We will present results for the mobility of short single-stranded DNA (ss-DNA) from experiments and from numerical simulations of a simple model system. For very short molecules ($\lesssim$20 bases) the molecules are mainly stretched and the (long-ranged) hydrodynamic interaction leads to an increase of the mobility with molecular size. Beyond 20 bases, however, the molecule starts to coil, and the driving and drag forces scale equally with the molecular size, leading to a constant mobility, i.e., the molecules behave now as free draining coils.[1]

Having established an understanding of the dynamics of short nucleic acids, we investigate the impact on their mobility when a neutral group is attached to one end of the molecules. As was suggested by Noolandi[4] for hybrid DNA−peptide molecules, this should lead to a different scaling of the drag force with molecular size, and this concept has been extended to suggest that single-base resolution sequencing of labeled single-stranded DNA up to 3000 bases using free solution electrophoresis and neutral proteins such as streptavidin as labels might be possible.[5]

Our focus is on short molecules (up to 40 bases) and small labels the size of a single nucleic acid (we used both biotin and a dimethoxytrityl modifications in the experiments) which can be considered as just another monomer unit on the polyelectrolyte, but with zero charge. For these short molecules with small neutral tails attached, we observe a shift of the mobilities from those of unlabeled DNA molecules, but the quantitative difference due to the increased overall friction coefficient decreases with increasing molecular size. However, for not too long nucleic acids (up to 40 bases) the impact of the additional neutral tail (which is the size of a nucleotide) on the mobility is significant enough to allow for a unique detection of both the labeled and unlabeled molecules.

The paper is organized as follows: In Section II we review some theoretical results on the electrophoretic mobility of a single polyelectrolyte molecule. In the next two sections we motivate our model for the numerical calculations and discuss the simulation results. The experimental setup is explained in Section V, and the results are presented in Section VI, including a com-

[⊗] Abstract published in *Advance ACS Abstracts,* November 1, 1995.

0024-9297/95/2228-8182$09.00/0

parison with the computer simulations. Section VII contains a brief summary and conclusions.

II. Theory

The electrophoretic mobility of a charged molecule is defined as the ratio of its steady-state velocity v_{ss} over unit electric field strength E:[1]

$$\mu = v_{ss}/E \tag{1}$$

In the case of diffusion dominated dynamics, eq 1 can "formally" be written as

$$\mu = \frac{F/E}{f} = \frac{q}{f} \tag{2}$$

where F is the force acting on the polyelectrolyte and q and f are the effective charge and the friction coefficient of the molecule, respectively. The counterions and possible buffer ions present in the solvent can influence both the effective charge on the molecule and its friction coefficient (by changing its average shape), quite strongly. Moreover, these ions introduce additional length and time scales which are important for the understanding of the dynamics of the charged molecule in an external electric field.

The electrophoresis of charged spheres has been studied extensively theoretically,[6-11] and a solution in the linear response regime for steady-state external fields and a centrosymmetric charge distribution has been derived. Similar work on cylinders is still approximate.[12]

For flexible molecules the situation becomes even more complicated, since the different parts of the electrolyte interact with each other through Coulomb and hydrodynamic forces (i.e., perturbations introduced in the solvent by one part of the polyelectrolyte will be transmitted through the fluid to other parts of the same molecule), both of which are long-ranged. Common approaches treat the solvent as an incompressible fluid and the polyelectrolyte as a chain of beads, interconnected by springs. Chain stiffness, which for large Debye lengths is enhanced by the repulsive Coulomb interaction between different beads, is enforced through a proper bending potential, characterized by a typical length scale called the *persistence length* (see, e.g., ref 13 and references therein).

Elvingson[14] performed molecular dynamics simulations on polyelectrolytes, considering explicitly *double-stranded* DNA (ds-DNA). In this work the effects of the counterions are incorporated by introducing an induced dipole moment of the molecule. For short ds-DNA (100−200 base pairs) he observed the molecules forming a U-shaped structure which aligned itself parallel to the applied external field. Further numerical simulations[14] and electro-optical experiments[16] seem to confirm these observations.

Experiments on *single-stranded* DNA in free solution electrophoresis show a strong increase of the mobility for short molecules (≤20 bases) before saturation sets in.[1] We have performed analytic calculations for stiff Gaussian molecules,[17] following a procedure motivated by Muthukumar.[18] Assuming freely rotating molecules (which seems to be a valid assumption in the case of short ss-DNA according to our numerical simulations), we calculated the electrophoretic mobility as function of molecular size and Debye length (i.e., counterion concentration). In the range of 100−1000 segments, the mobility can be described very well by a simple power

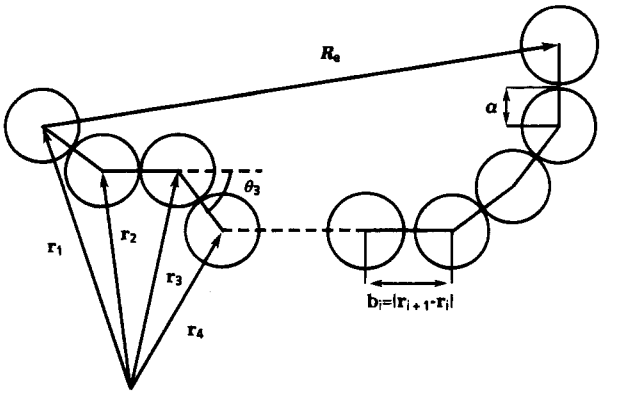

Figure 1. Model molecule; the neighboring beads do not necessarily touch each other due to the harmonic stretching potential between them.

law. The value of the exponent varied between 0.5 for the Gaussian chain at infinite Debye length and ≈0 for the rigid rod-like molecule at zero Debye length, but its dependence on the Debye length for a fixed stiffness was quite independent on the value of the stiffness. These calculations suggest that for not too stiff polyelectrolytes and low counterion concentration the increase of the mobility with molecular size is big enough to be detected in experiments. However, ss-DNA is quite stiff, and typical buffer solutions used in electrophoresis contains a rather high counterion concentration (cf. Grossman),[1] hence leading to the observation of an almost size-independent mobility beyond about 20 bases.

In the case of constant mobility (i.e., μ does not depend on the size of the molecules), the effective charge and the friction coefficient both scale equally with the molecular size L:

$$\mu = \frac{Lq_0}{Lf_0} = \frac{q_0}{f_0} \tag{3}$$

(q_0 and f_0 are the effective charge and friction coefficient of a single segment, respectively). To achieve a separation of these polyelectrolytes by electrophoresis, one has to break this scaling symmetry, which can be accomplished in several ways. In the present work, we investigate the effect of a neutral end group the size of approximately one base on the mobility. The additional friction is in zeroth order independent on the size of the molecule, hence leading to a breaking of the above scaling:

$$\mu = \frac{Lq_0}{Lf_0 + f_c} = \frac{q_0}{f_0 + f_c/L} \tag{4}$$

where f_c is the additional friction coefficient due to the neutral end label. The influence of this neutral end group is supposed to be rather strong for shorter polyelectrolytes, but becomes less important with increasing molecular size. Another way to break the scaling symmetry (eq 3) is to locally change the stiffness of the polyelectrolyte. Possibilities, how to achieve this, and where this technique might be useful, will be discussed in a forthcoming article.

III. Numerical Simulation Procedure

We consider a discrete worm-like chain model with N beads of radius a which are linked together by $N - 1$ springs (Figure 1). We use a Brownian dynamics algorithm to calculate the time evolution of single

chains. With the N beads at positions $\mathbf{r}_i$, $i = 1 ..., N$, the equations of motion are[19]

$$\dot{\mathbf{r}}_i = \sum_{j=1}^{N} \mathbf{D}_{ij}\mathbf{F}_j + \mathbf{N}_i(t) \tag{5}$$

$\mathbf{F}_j$, the direct force acting on bead j, is the sum of the external electric force

$$\mathbf{F}_j^{\mathrm{e}} = q_j\mathbf{E} \tag{6}$$

and the interchain forces due to the bending (U^{b}) and stretching (U^{s}) potentials:[20]

$$U^{\mathrm{b}} = \frac{g}{2}\sum_{j=1}^{N-2} \theta_j^{\,2} \tag{7}$$

$$U^{\mathrm{s}} = \frac{h}{2}\sum_{j=1}^{N-1} (b_j - 2a)^2 \tag{8}$$

where θ_j is the angle between the virtual bonds j and $j + 1$. The strength of the bending potential g is related to the persistence length P by the expression

$$g = \frac{Pk_{\mathrm{b}}T}{b} \tag{9}$$

with $b = 2a$ is the equilibrium bond length. The $\mathbf{N}_i(t)$ are Gaussian distributed random numbers with zero mean and variance

$$\langle \mathbf{N}_i(t)\, \mathbf{N}_j(t')\rangle = 2k_{\mathrm{B}}T\mathbf{D}_{ij}\delta(t - t') \tag{10}$$

The tensor $\mathbf{D}_{ij}$ includes the self-diffusion of the beads

$$\mathbf{D}_{ii} = \frac{1}{6\pi\eta a}\mathbf{I} \tag{11}$$

where η is the solvent viscosity and $\mathbf{I}$ is the 3×3 unit tensor, and the hydrodynamic interactions (HI), for which we use the approximation of Rotne and Prager[21] for no-slip boundary conditions

$$\mathbf{D}_{ij} = \begin{cases} \dfrac{1}{8\pi\eta r_{ij}}\left[\mathbf{I} + \dfrac{\mathbf{r}_{ij}\mathbf{r}_{ij}}{r_{ij}^{\,2}} + \dfrac{2a^2}{r_{ij}^{\,2}}\left(\dfrac{1}{3}\mathbf{I} - \dfrac{\mathbf{r}_{ij}\mathbf{r}_{ij}}{r_{ij}^{\,2}}\right)\right] & r_{ij} \geq 2a \\ \dfrac{1}{6\pi\eta a}\left[\left(1 - \dfrac{9}{32}\dfrac{r_{ij}}{a}\right)\mathbf{I} + \dfrac{3}{32}\dfrac{\mathbf{r}_{ij}\mathbf{r}_{ij}}{ar_{ij}}\right] & r_{ij} < 2a \end{cases} \tag{12}$$

with $\mathbf{r}_{ij} = \mathbf{r}_i - \mathbf{r}_j$.

For our simulations we choose the beads to be the size of a single base, i.e., $a = 0.17$ nm (estimated from the size of base pairs in ds-DNA),[20] which is big enough to avoid the additional degrees of freedom which are not relevant for the time scales of interest, but small enough to mimic properly the shape-dependent overall friction coefficient.

The presence of counterions in the solvent influences the dynamics of the polyelectrolyte, but an explicit treatment of these ions within the numerical simulations is nearly impossible presently due to the required computer resources. On the other hand, if the counterion concentration is high, they are mainly distributed near the backbone of the polyelectrolyte, and the approximation of spherical distributed counterion clouds around each bead of the model polyelectrolyte with a typical width of the Debye length λ is a valid approach to simplify the complicated dynamics of the system. Analytical calculations within this approximation show that an increase of the counterion concentration leads to a saturation of the mobility beyond a certain molecular size due to a cancelation of the long-range hydrodynamic interactions through the long-range Coulomb interactions of the counterions (which in the above approximation are described by a Debye–Hückel potential).[17] An increase of the polyelectrolyte stiffness (for fixed counterion concentration) leads also to a saturation of the mobility beyond a certain molecular size regime, but in this case it is due to the increase of the prolateness of the shape of the stiffer molecules, which for free rotation leads to a larger average cross section of the molecule while moving through the solvent. In order to keep the simulation time manageable, we performed our numerical simulations with no counterions (i.e., $\lambda \to \infty$), but with a finite persistence length $P = 5b$. This approximation severely limits the possibility to quantitatively compare the simulation results with the experiments. On the other hand, we believe that this simple model is sufficient to explain the crucial contributions to the polyelectrolyte dynamics, while the counterions present in the experiment mainly lead to a stronger saturation of the mobility with increasing molecular size.

After finishing most of the simulations presented here, we learned that ss-DNA has a persistence length of $P \cong 4...5$ nm or $P \cong 10...15b$, as determined by transient birefringence experiments.[22]

An integration step of $\mathrm{d}t = 2$ ps is used which is long enough to allow for momentum relaxation within each time step, but which is still within the time scale of the typical bending mode between two adjacent beads, allowing us to follow the long-time scale conformational changes.

Typical experimental values for the applied electric field are of the order of 10^2 V/cm. Considering an effective base charge of $q = -e$, this results in a position displacement $(\Delta r)_{\mathrm{el}}$ per integration step which is a factor of 10^5 smaller than the average position displacement of a bead due to noise $(\Delta r)_{\mathrm{noise}}$. To obtain reliable data for the mobility in this case, we would have to perform rather lengthy calculations. Therefore, we use for the present simulations a value of $E = 10^4$ V/cm. Within our model, this leads to a higher steady-state velocity (which is linear in E) and to a smaller ratio of $(\Delta r)_{\mathrm{el}}$ and $(\Delta r)_{\mathrm{noise}}$. This allows us to estimate the electrophoretic mobility with less time-consuming numerical simulations.

Equation 5 is integrated explicitly, using a second order Runge Kutta method for stochastic differential equations.[23,24] Initial configurations are randomly generated using a random-ϕ model with the interbond angle distribution given by[25]

$$\phi(\theta_j) \propto \sin\theta_j \exp(-P\theta_j^{\,2}/b) \tag{13}$$

and fixed bond length b.

IV. Numerical Results

A. Unlabeled Polyelectrolytes. Our choice of $P = 5b$ for the persistence length leads to rather stiff molecules (though it appears to be more flexible than ss-DNA,[22] but it is much more flexible than ds-DNA), where the shorter molecules have a pronounced elongated shape. Figure 2 shows snapshots of molecular conformations for 10- and 25-bead chains. During 60

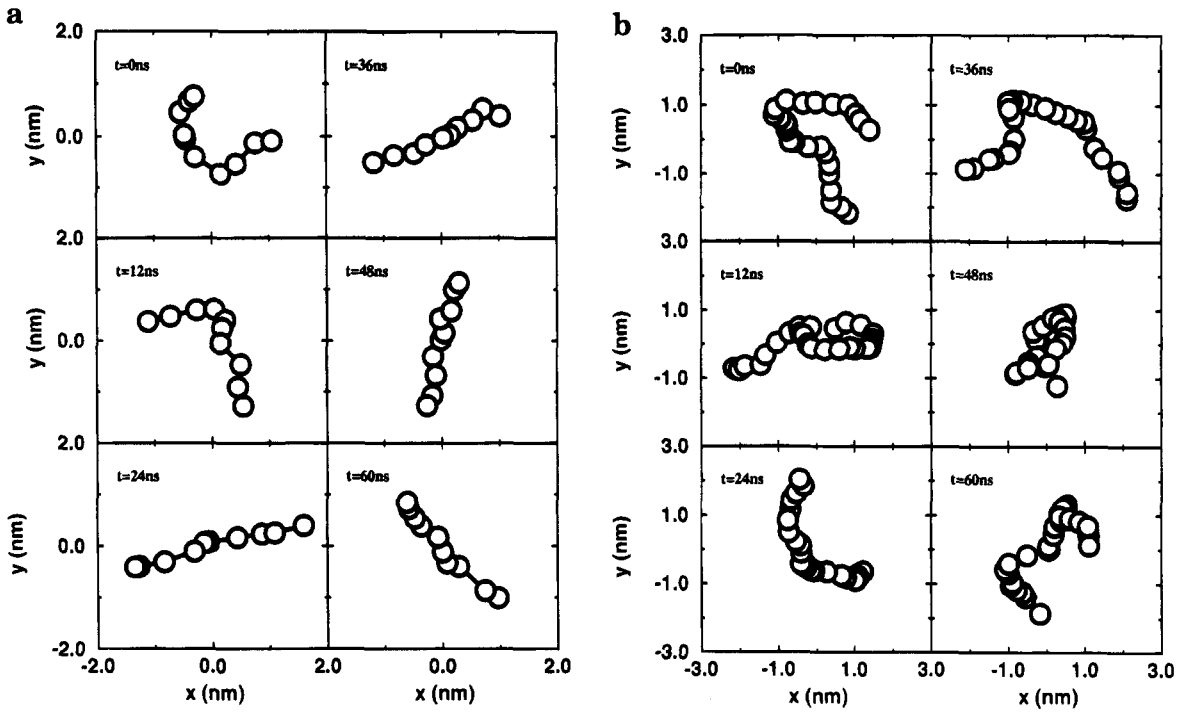

Figure 2. Snapshots of chain configurations during numerical simulations for molecules with (a) 10 and (b) 25 beads. The origin of the coordinate system is fixed to the center of mass of the model polyelectrolytes.

ns (i.e., 30 000 integration steps), the orientation of the molecules has changed completely, while the center of mass has moved on the order of 100 times the total molecular size due to the electric field. This lack of a preferred orientation of the molecules is also reflected in the orientational order parameter[26]

$$S = \frac{3}{2}\left\langle (\mathbf{u}\cdot\mathbf{n})^2 - \frac{1}{3}\right\rangle \qquad (14)$$

where $\mathbf{n}$ and $\mathbf{u}$ are unit vectors parallel to the electric field and the molecule's longest axes, respectively. In all our simulations S is always zero when averaged over a sufficiently long time period. In contrast to ds-DNA, where orientational effects have been observed, both experimentally[16] and numerically,[14,15] we find the single-stranded model DNA molecules rotate freely around themselves while moving against the electric field. This is probably an effect of the smaller bead size in the investigated system, which leads to a larger influence of the Brownian forces on the molecular dynamics (and which is rather independent of the actual persistence length of the polyelectrolyte).

The data for the mobility obtained from the numerical simulations are shown in Figure 3 (circles). For short chains ($L \leq 15$) μ is increasing rather strongly before it slowly starts to saturate. The bend in the mobility curve at $N = 30$ has been discussed in ref 17. The solid line in Figure 3 shows the result from analytic calculations for the stiff Gaussian chain,[17] which is systematically larger than the mobility from the numerical simulation. The two different models, however, seem to produce qualitatively different results for μ only for small molecules (up to $L \approx 25b$), where the difference between the mobilities of the two models increases with molecular size, while for longer molecules both models seem to scale equally with L (cf. ref 17). The main difference between the two models is in the average segment length, which is zero in the stiff Gaussian chain model, but finite (b) in the computer model.

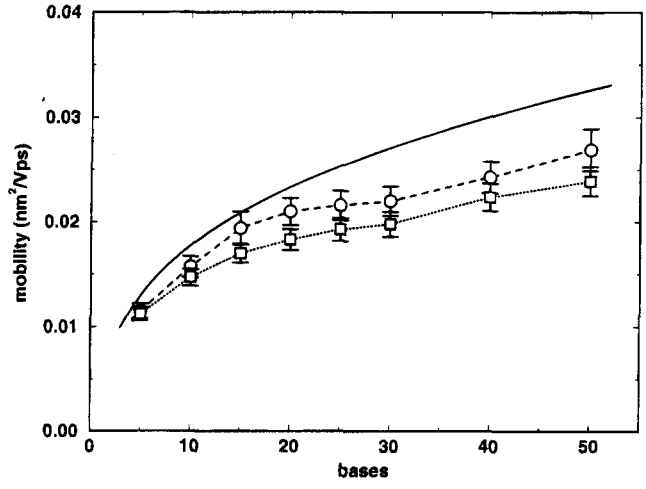

Figure 3. Mobility as function of molecular size: (○) results of full simulations; (□) mobility using preaveraged diffusion tensor; —, analytic mobility of a stiff Gaussian chain[17] (dashed and dotted lines are only guides for the eye).

The simulations discussed so far have all been performed with the diffusion tensor $\mathbf{D}_{ij}$ being updated for each time step, using a Cholesky factorization[27] to calculate the noise amplitudes. This procedure becomes very computationally time consuming for longer molecules, not only because of the larger number of beads, but also because longer simulation runs are required due to the longer time scales of the intramolecular dynamics. The free rotation of the molecules about themselves suggests the use of an orientationally preaveraged diffusion tensor. Following the scheme of ref 20, we calculated the average diffusion tensor from randomly generated chains. The procedure was terminated when the error of each of the components of the tensor was less than one per million. The random chains were generated the same way as the initial conditions for the simulations; i.e., the interbond angles were selected from the distribution for the random-ϕ model (eq 13). For most of the cases considered, we used a fixed bond

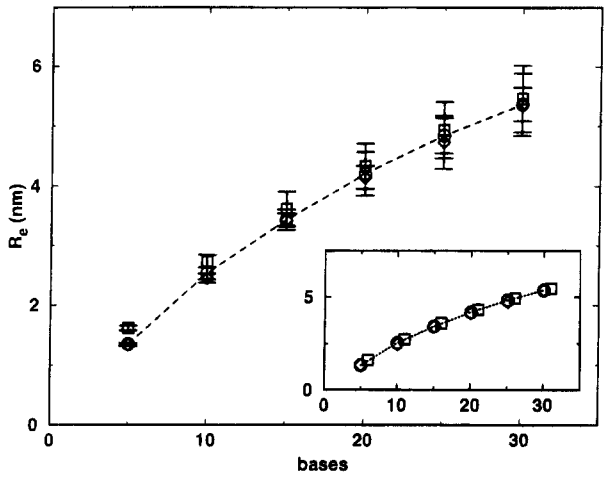

Figure 4. End-to-end distance as function of molecular size: ○, unlabeled molecule, full simulations; □, unlabeled molecule, preaveraged diffusion tensor (using the same persistence length as in the dynamics simulations); ◇, labeled molecule, full simulation. The inset shows the same data, but with the data of the labeled molecules shifted to the right by 1. The dashed line corresponds to the Kratky–Porod result, eq 15.

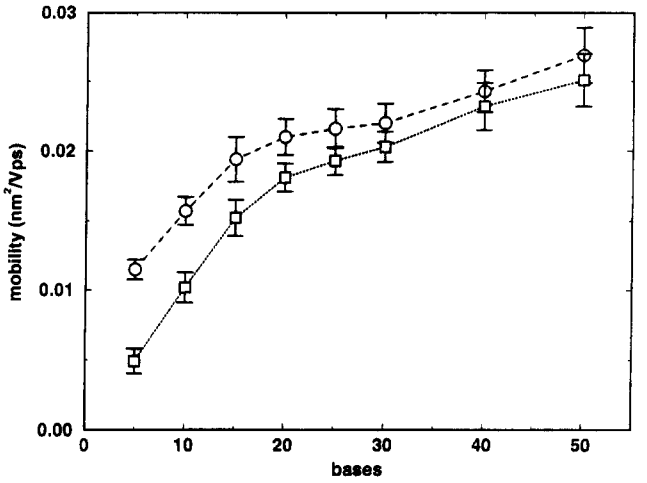

Figure 5. Mobility as function of molecular size: ○, unlabeled molecule; □, labeled molecule; the lines are only guides to the eye.

length b, since a more general approach with bond lengths b_i selected from a Gaussian distribution with mean value b and variance $\langle(b_i - b)^2\rangle = k_BT/h$ did not lead to significantly different results.

The simulation data using the preaveraged diffusion tensor for the mobility (μ_p) are compared with the results of the full simulations in Figure 3. We find μ_p to be approximately equal to μ for $N \lesssim 15$, before the mobility of the model using the preaveraged diffusion tensor becomes systematically smaller than μ. This is due to the average value of the HI, which does not properly take into account its nonlinear dependence on the interbead distances. The mobility of a coiled molecule is appreciably higher than for a stretched one due to the HI. This results in a higher average speed than using the preaveraged diffusion tensor which no longer reflects the actual shape of the polyelectrolyte. As a result, we observe a smaller mobility using this preaveraged diffusion tensor.

In contrast to the mobility, which is a dynamic property of the system, we do not see a significant or systematic deviation of the averaged end-to-end distance of the simulations with preaveraged diffusion tensor (independent of the method to generate it) from the data of the full simulations (Figure 4). The dashed line shows the Kratky–Porod result for the averaged end-to-end distance of a stiff Gaussian chain[28]

$$R_e^2 = 2LP - 2P^2(1 - e^{-L/P}) \qquad (15)$$

which agrees very well with our numerical simulations.

B. Polyelectrolytes with a Neutral Label. The simulations for polyelectrolytes with a neutral end group were performed in the same way as those for the unlabeled molecules. For convenience, we treated the neutral label as an additional base with the same properties as all the others (size, coupling to chain, etc.), but set its charge to zero. Thus, the bending and stretching forces and the HI are identical throughout the whole molecule. In the limit of infinite Debye length, there is no influence of the neutral end group upon the electric force acting on the charged segments. Therefore, by adding the neutral tail, we increase the overall friction coefficient of the molecule, while keeping the total dragging force constant.

In Figure 5 we compare the mobility of model polyelectrolytes with and without a neutral label. In both cases we plot the mobility as function of the number of negatively charged segments. For most of the molecular sizes under consideration, there is no qualitative change of the mobility μ_n of the molecules with additional neutral tail. We observe a strong increase of μ_n for $L \lesssim 20b$ before it starts to saturate. Because of the larger overall friction coefficient, the mobility in this case is systematically smaller than for the molecules without a tail, but the mobilities for both cases approach each other with increasing size. We also observe the molecules rotating freely around themselves, independent of the tail. As a result, we find that attaching a neutral label does not qualitatively change the dependence of the mobility of flexible polyelectrolytes on the molecular size, where there is saturation of the mobility beyond a certain molecular size. However, the absolute mobility of a labeled polyelectrolyte of a given length is clearly distinguishable from the value of μ for an unlabeled molecule up to $N \approx 25$. This effect might prove useful for diagnostic purposes.

The averaged end-to-end distance is shown in Figure 4. The R_e's of chains with neutral tail are systematically larger than those for the plain molecules. However, if we plot the R_e as function of the total number of segments per molecule, the data for both types of molecules fit onto the same line (cf. inset of Figure 4); thus, the molecular conformations are basically independent of the charge of the single beads for the electric field used in the calculations.

V. Materials and Methods

A. Instrumentation. Capillary electrophoretic separations were carried out on a Beckman Instruments (Beckman Instruments, Fullerton, CA) Model 2000 P/ACE capillary electrophoresis system equipped with a 87 cm fused silica capillary with 75 μm i.d. and 365 μm o.d. (Polymicro Technologies, Phoenix, AZ). The DNA samples were detected at 260 nm using an on-column UV absorbance detector. Electrophoretic separation of ss-DNA was achieved with 10 mM $Na_2B_4O_7$ as the running buffer and an applied voltage of 10 kV. The DNA samples were detected at 260 nm using an on-column UV absorbance detector. A sample solution

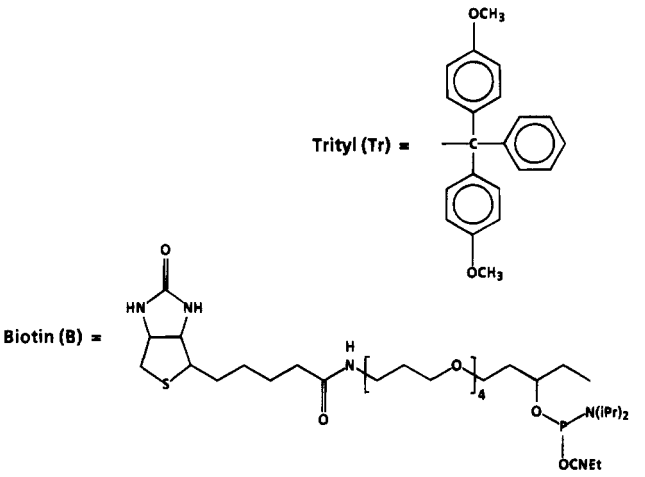

Figure 6. Chemical structures of biotin and trityl modifications used as neutral labels on the single-stranded DNA.

Table 1. Sequences of ss-DNA Used in the Experiments[a]

19mer:	5'GGG TGT TTT GGT GTG TTG3'
19mer + B:	5'BGG GTG TTT TGG TGT GTT G3'
29mer:	5'GGG TGT TTT GGT GTG TTG GGG TGT TTT G3'
29mer + B:	5'BGG GTG TTT TGG TGT GTT GGG GTG TTT TG3'
41mer:	5'AGA TCT AGA GGA GAC CCC ACA TGC TTT CCC CGG ACG AGC AG3'
41mer + Tr:	5'TrAG ATC TAG AGG AGA CCC CAC ATG CTT TCC CCG GAC GAG CAG3'
42mer:	5'AGA TCT AGA GGA GAC CCC ACA TGA CCG AGG TGG ACG GGC GCA3'
42mer + Tr:	5'TrAG ATC TAG AGG AGA CCC CAC ATG ACC GAG GTG GAC GGG CGC A3'

[a] Biotin (B) and trityl (Tr) groups are on the 5' end. All samples are provided by Al Smith of the P/AN facility, Stanford.

was introduced hydrodynamically for 1.0 s into the capillary. The electropherograms were acquired using P/ACE system software furnished by Beckman Instruments.

B. Sample and Reagents. 1. Chemicals. Sodium tetraborate decahydrate (10 mM, pH 9.1) was purchased from Aldrich Chemicals (Milwaukee, WI) and used as the running buffer throughout. Water was triply distilled and deionized. 4-Methyl-3-penten-2-one (mesityl oxide) was obtained from Aldrich Chemicals (Milwaukee, WI). Buffer solutions were filtered through a 0.45 μm pore size filter (Millipore, USA).

2. Oligonucleotides. Singe-stranded oligonucleotides of varying lengths were synthesized on an Applied Biosystems DNA synthesizer (ABI, San Jose, CA) at the P/AN Facility (Stanford University, Stanford, CA) using standard phosphoramidite chemistry. Biotin and dimethoxytrityl modifications (Figure 6) were done on the 5' end of the DNA strands. The synthesized DNA strands were dissolved in 1× TBE and stored at 0 °C. Table 1 lists the DNA strands used for our experiments.

C. Procedures. 1. Capillary Conditioning. Prior to each day of analysis, the fused-silica capillary was pretreated with a 100 mM sodium hydroxide solution for 5 min, followed by 5 min each of distilled water and buffer. At the end of each day, the capillary was flushed

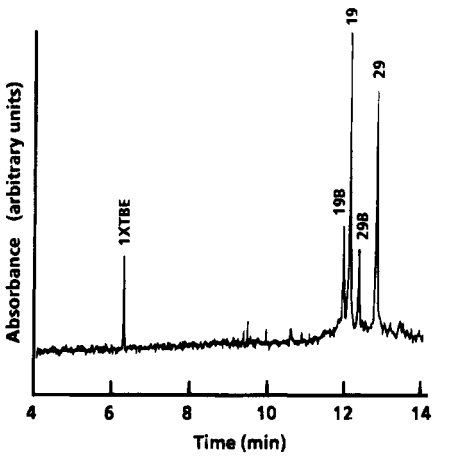

Figure 7. Electropherogram of 19- and 29-mer nucleic acids without and with biotin (B) attached to the 5' end obtained in free solution; including neutral peak (1× TBE).

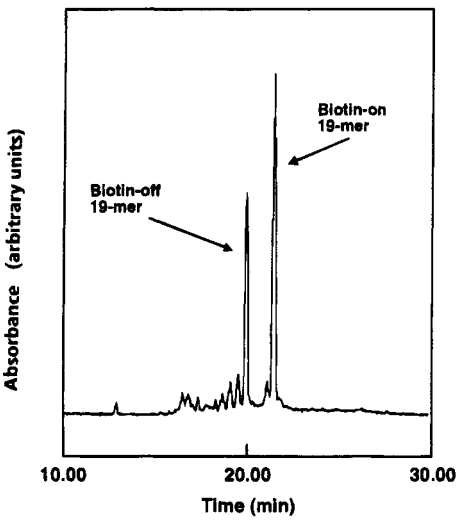

Figure 8. Electropherogram of a 19-mer nucleic acid without and with (biotin) label obtained by capillary gel electrophoresis.

with buffer. All solutions were flushed through the capillary by vacuum.

2. Free Solution Capillary Electrophoresis. In all experiments a nonionized molecule, mesityl oxide, was used as the electroosmotic flow marker. The DNA samples were introduced into the capillary inlet by hydrodynamic injection for 1 s. The separations were driven using a voltage of 20 kV (230 V/cm, approximately 22 μA, 25 °C). The positions of unmodified DNA samples in the electropherograms of mixed DNA samples were determined by spiking the sample with the approximately pure DNA strand.

VI. Experimental Results and Comparison with Computer Simulations

Free solution capillary electrophoresis data are shown in Figures 7 and 8. In these experiments, the nucleic acid molecules move against the electroosmotic flow of the solvent induced by the positively charged buffer ions next to the capillary wall. The velocity of the electroosmotic flow is larger than the electrophoretic velocity of the DNA molecules; hence, they move in the same direction as the solvent, but their net velocity is smaller for a higher electrophoretic mobility.

Figure 7 shows the electropherograms of 19- and 29-mers with and without biotin label. These two oligomers have been designed by using nucleotides with

thymine and guanine as bases only to avoid hybridization of the ss-DNA fragments with themselves. For ss-DNA with 41 and 42 bases, the mobilities are about the same, though the larger molecules are still slightly faster (Figure 8). Though both the 41- and 42-mers contain all four different bases, possible hybridization between different molecules does not appear to be a problem.

Nucleic acids with a neutral tail have a systematically smaller mobility, independent of whether we use biotin (Figure 7) or trityl (Figure 8). While for the shorter chains the molecules with an attached neutral tail show up in a clearly separated peak in the electropherograms, this is no longer true for the longer chains, where we observe quite a strong overlap. This reduction of the difference of the mobility between the unlabeled and the labeled DNA has also been observed in our numerical simulations (Figure 4). Though the fact that the labeled molecules should have a smaller mobility seems to be obvious, it indicates that our simple numerical model is sufficient to describe the main dynamics of the polyelectrolyte. Especially, any induced dipole moments due to the presence of counterions in the solvent do not lead to an alignment of the molecules parallel to the electric field, as has been observed for ds-DNA, both in simulations[14] and in recent experiments.[15] An alignment of the polyelectrolyte with the field improves the "aerodynamics" of the molecule within the solvent and leads to an increase of the mobility. This is even true for the labeled polyelectrolytes, though the neutral end label breaks the charge symmetry on the molecule.

This dominance of the Brownian forces on the polyelectrolyte dynamics is likely the main reason why neglecting the counterions does not lead to a qualitatively different dynamics between the numerical model and the experiment.

By increasing the size of the polyelectrolyte and/or the size of the neutral label, the Brownian forces become less dominant and the polyelectrolyte dynamics may change. In this case, the breaking of the charge symmetry may lead to an orientation of the polyelectrolyte parallel to the field. The increase of the mobility due to hydrodynamics would balance the increased friction due to the neutral label and would limit the possibility of single base resolution sequencing of protein-labeled DNA in free solution.[5] Experiments and/or more detailed theoretical investigations for these systems will be necessary to clarify its usefulness for sequencing.

Control experiments with the same molecules using *capillary gel electrophoresis* are shown in Figures 9 and 10 for the 19-mer and the 40/41-mers, respectively. In this case, there is no electroosmotic flow of the solvent, and hence the molecules with the highest mobilities are detected first. Again, we observe a higher mobility for the unlabeled molecules, but the difference to the mobility of the labeled molecules is decreasing with increasing molecular size. The gel electrophoresis experiments need an appreciably longer amount of time due to a systematically smaller speed of the polyelectrolytes; however, the resulting bands are much sharper, which allows for a clear separation of the labeled from the unlabeled molecules even for the largest oligomers used in our investigation.

VII. Conclusions

We have performed numerical simulations and free solution capillary electrophoresis experiments on the mobility of short single-stranded nucleic acid molecules.

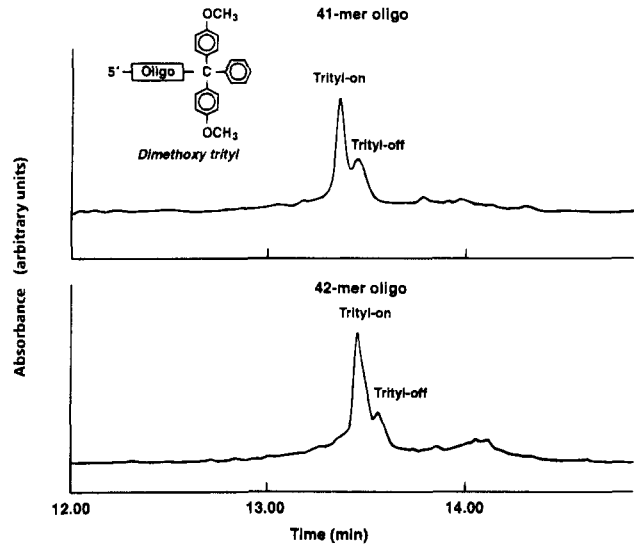

Figure 9. Electropherograms of 40- and 41-mer nucleic acids in free solution without and with (trityl) label.

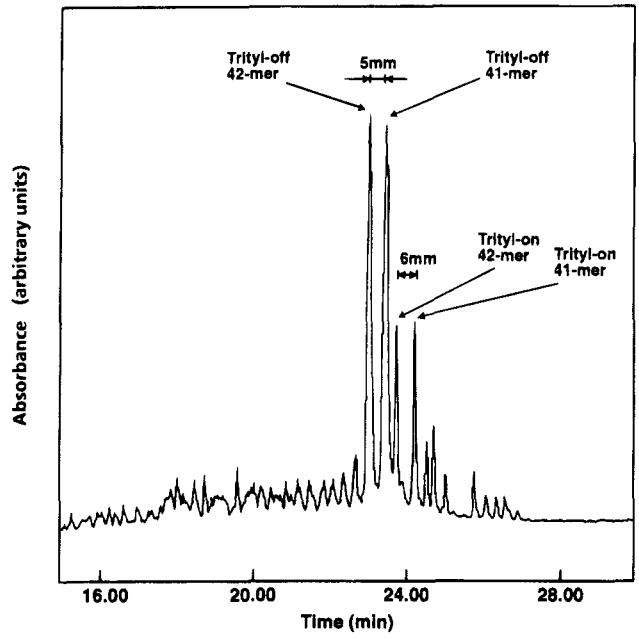

Figure 10. Electropherograms of 40- and 41-mer nucleic acids without and with (trityl) label obtained by capillary gel electrophoresis.

Comparison of the simulation data for the mobility with experimental results shows good qualitative agreement, i.e., the mobility increases rather strongly for very short molecules, but starts to saturate above about 20 bases. The simulations indicate that the molecules in all cases considered rotate freely about themselves during the electrophoresis. This is in contrast to experimental results for double-stranded DNA, where an alignment of the molecules parallel to the applied electric field has been observed,[15] and the corresponding numerical simulations showed a partial alignment even without taking the polarization effects of the counterion sphere into account.[14] In the case of single-stranded DNA, however, the Brownian force seems to dominate over the hydrodynamic and possible dipolar interactions, leading to a random orientation of the molecules.

Attaching short neutral tails (biotin, trityl) to the negatively charged nucleic acid molecules leads to a systematic smaller mobility due to the larger overall friction coefficient. The qualitative dependence of the

mobility on the molecular size is the same for labeled and unlabeled molecules, and the difference between their mobilities decreases with increasing molecular size.

The good agreement between our simple numerical model and experimental results appears to be due to the dominance of Brownian forces on the polyelectrolyte dynamics. By increasing the polyelectrolyte and/or end label size, the Brownian forces become less important, and a more extended model system, which includes counterion dynamics, might be necessary for a realistic description.

Gel electrophoresis experiments using the same oligomers need more time than the capillary free solution electrophoresis experiments due to a smaller overall migration speed of polyelectrolytes in restricted media, but, on the other hand, the peaks are better separated and sharper. Moreover, gel electrophoresis provides a well-established tool to separate ss-DNA up to a few hundred bases with single-base resolution, whereas there is no size dependence of the free solution mobility of flexible polyelectrolytes beyond a few bases. Recent suggestions to utilize free solution electrophoresis for DNA sequencing by using protein–DNA complexes still wait for experimental proof. However, we have demonstrated that rather small changes in the physical properties of a polyelectrolyte (e.g., a single neutral segment out of 25 charged ones) can lead to a significant shift in the free solution mobility. This might be used as a diagnostic tool to detect ss-DNA fragments with well-specified properties in free solution by selectively changing their physical properties.

Acknowledgment. We wish to thank Dr. M. Dulay and Prof. R. Zare for providing us with the experimental data and many helpful discussions. One of us (A.R.V.) acknowledges a postdoctoral fellowship of the Deutsche Forschungsgemeinschaft.

References and Notes

(1) Grossman, P. D. In *Capillary Electrophor.* **1992**, 111.
(2) Noolandi, J. *Adv. Electrophor.* **1992**, *5*, 1.
(3) Grossman, P. D. *J. Chromatogr.* **1994**, *663*, 219.
(4) Noolandi, J. *Electrophoresis* **1993**, *14*, 680.
(5) Mayer, P.; Slater, G. W.; Drouin, G. *Anal. Chem.* **1994**, *66*, 1777.
(6) Hückel, E. *Physik. Z.* **1924**, *25*, 204.
(7) Onsager, L. *Physik. Z.* **1926**, *27*, 388.
(8) Onsager, L. *Physik. Z.* **1927**, *28*, 277.
(9) Wiersema, P. H.; Loeb, A. L.; Overbeek, J. Th. G. *J. Colloid Interface Sci.* **1966**, *22*, 78.
(10) O'Brien, R. W.; White, L. R. *J. Chem. Soc., Faraday Trans. 2* **1978**, *74*, 1607.
(11) Allison, S. A.; Nambi, P. *Macromolecules* **1992**, *25*, 3971.
(12) Hunter, R. J. *Zeta Potentials in Colloid Science*; Academic Press: New York, 1981.
(13) Stevens, M. J.; Kremer, K. *ACS Symp. Ser.* **1994**, *548*, 57.
(14) Elvingson, C. *Biophys. Chem.* **1992**, *43*, 9.
(15) Allison, S. A. *Macromolecules* **1993**, *26*, 4715.
(16) Antosiewicz, J.; Porschke, D. *Biophys. Chem.* **1989**, *15*, 263.
(17) Völkel, A. R.; Noolandi, J. *J. Chem. Phys.* **1995**, *102*, 5506.
(18) Muthukumar, M. *Macromol. Theory Simul.* **1994**, *3*, 61.
(19) Fixman, M. *Macromolecules* **1986**, *19*, 1195.
(20) Allison, S. A. *Macromolecules* **1986**, *19*, 118.
(21) Rotne, J.; Prager, S. *J. Chem. Phys.* **1969**, *50*, 4831.
(22) Weill, G. Private communication.
(23) Helfand, E. *Bell Syst. Techn. J.* **1979**, *58*, 2289.
(24) Greenside, H. S.; Helfand, E. *Bell Syst. Tech. J.* **1981**, *60*, 1927.
(25) Hagerman, P. J.; Zimm, B. H. *Biopolymers* **1981**, *20*, 1481.
(26) Doi, M.; Edwards, S. F. *The Theory of Polymer Dynamics*; Clarendon Press: Oxford, 1986.
(27) Dahlquist, G.; Björck, Å. *Numerical Methods*; Prentice-Hall: Englewood Cliffs, 1974.
(28) Kratky, O.; Porod, G. *Recl. Trav. Chim.* **1949**, *68*, 1106.

MA950609Y